



Published in final edited form as:

Nature. 2017 October 12; 550(7675): 214–218. doi:10.1038/nature23907.

## The transcription fidelity factor GreA impedes DNA break repair

Priya Sivaramakrishnan<sup>1</sup>, Leonardo A. Sepúlveda<sup>2</sup>, Jennifer A. Halliday<sup>1</sup>, Jingjing Liu<sup>1</sup>, María Angélica Bravo Núñez<sup>1</sup>, Ido Golding<sup>2,3</sup>, Susan M. Rosenberg<sup>1,2,3,4</sup>, and Christophe Herman<sup>1,3,4,\*</sup>

<sup>1</sup>Department of Molecular and Human Genetics, Baylor College of Medicine, Houston, TX 77030, USA

<sup>2</sup>Verna and Marrs McLean Department of Biochemistry and Molecular Biology, Baylor College of Medicine, Houston, Texas 77030, USA

<sup>3</sup>Dan L. Duncan Comprehensive Cancer Center, Baylor College of Medicine, Houston, TX 77030, USA

<sup>4</sup>Department of Molecular Virology and Microbiology, Baylor College of Medicine, Houston, Texas 77030, USA

### Abstract

Homologous recombination repairs DNA double-strand breaks and must function even on actively transcribed DNA. Because break repair prevents chromosome loss, the completion of repair is expected to outweigh the transcription of broken templates. Yet, the interplay between DNA break repair and transcription processivity is unclear. Here we show that the transcription factor GreA inhibits break repair in *Escherichia coli*. GreA restarts backtracked RNA polymerase (RNAP) and hence promotes transcription fidelity. We report that removal of GreA results in dramatically enhanced break repair via the classical RecBCD-RecA pathway. Using a deep-sequencing method to measure chromosomal exonucleolytic degradation (XO-Seq), we demonstrate that the absence of GreA limits RecBCD-mediated resection. Our findings suggest that increased RNAP backtracking promotes break repair by instigating RecA loading by RecBCD, without the influence of canonical Chi signals. The idea that backtracked RNAP can stimulate recombination

---

Users may view, print, copy, and download text and data-mine the content in such documents, for the purposes of academic research, subject always to the full Conditions of use: [http://www.nature.com/authors/editorial\\_policies/license.html#terms](http://www.nature.com/authors/editorial_policies/license.html#terms) Reprints and permissions information is available at [www.nature.com/reprints](http://www.nature.com/reprints)

\*Correspondence and requests for materials should be addressed to Christophe Herman ([herman@bcm.edu](mailto:herman@bcm.edu)).

#### Author contributions

P.S. and C.H. conceived the study. P.S., J.A.H., J.L. performed the experiments. M.A.B.N. and L.A.S. analyzed the sequencing data. L.A.S. and I.G. performed the mathematical modeling of RecBCD. P.S., C.H., L.A.S., I.G. and S.M.R. wrote the manuscript.

The authors declare no competing financial interests.

Supplementary Information is available in the online version of the paper at [www.nature.com/nature](http://www.nature.com/nature).

#### Data availability

Source data for main figures are provided with the paper. Raw data for Extended Data Figures are available from the corresponding author upon request.

#### Code Availability

MATLAB and R code available on reasonable request.

#### Accession codes

Sequencing data available through the SRA (SRP091869).

presents a DNA transaction conundrum: a transcription fidelity factor compromises genomic integrity.

---

DNA double-strand breaks (DSBs) are a potentially lethal form of damage and a source of genomic instability. Homologous recombination is essential for DSB repair and plays an important role in bacterial adaptation and genome evolution<sup>1</sup>. In *Escherichia coli*, DSB repair is initiated by the RecBCD enzyme. RecBCD resects DNA ends, degrading it into ssDNA and also loads the recombinase RecA to promote strand exchange<sup>2</sup>. RecBCD binds blunt DNA ends and translocates along the DNA while unwinding and degrading both strands<sup>3</sup> (Extended Data Fig. 1a). RecBCD switches from DNA degradation to RecA loading at distinct DNA sequences known as Chi sites<sup>4</sup>. Purified RecBCD is a powerful helicase that dislodges most DNA bound proteins<sup>5</sup>. However, some collisions between RNA polymerase (RNAP) and RecBCD result in stalling of the resection enzyme<sup>5</sup>. Transcription-coupled DNA repair (TCR) of helix-distorting lesions promoted by transcription elongation factors have been previously described<sup>6,7</sup> (Extended Data Fig. 1b). Here we show that the control of RNAP backtracking by these factors impairs DNA break repair by affecting RecBCD resection and consequently RecA loading at sites far removed from the original DNA break.

### Loss of GreA confers DSB-resistance in *E. coli*

RNAP backtracking can occur due to ribonucleotide misincorporation<sup>8</sup> or transcription encounters with helix-distorting DNA lesions<sup>7</sup>. During backtracking, the nascent mRNA is displaced from the RNAP active site into the secondary channel preventing transcription elongation<sup>9</sup> (Extended Data Fig. 1c). The GreA and GreB factors restart backtracked RNAP by stimulating RNA cleavage<sup>10</sup>, realigning the 3' end of the transcript with the active site, allowing transcription to resume<sup>9</sup> (Extended Data Fig. 1c). To determine if RNAP backtracking influences DNA break repair, we examined the DSB survival phenotypes of *gre* mutants upon exposure to the radiomimetic drug, phleomycin. Deletion of *greA* (*greA*) made cells highly resistant to phleomycin (Figs. 1a, b). The *greA*(D41N) allele that is disrupted for transcript cleavage activity<sup>11</sup> was also phleomycin resistant, indicating that impairment of the transcript cleavage function of GreA was sufficient for improved DSB survival. Loss of GreA did not affect break generation (Extended Data Fig. 2a). Deletion of *greB* caused no significant change in phleomycin sensitivity (Fig. 1b), but the *greB greA* double mutant was as resistant to phleomycin as the *greA* mutant (Fig. 1b). GreA and GreB have similar functions but differ in transcript cleavage specificity. GreA cleaves di- and trinucleotides arising from misincorporation, whereas GreB stimulates the cleavage of larger fragments<sup>10</sup>. Thus, the phleomycin survival difference between the *gre* mutants could be attributed to the differential transcript cleavage activity, suggesting that short RNAP backtracking due to misincorporation may enhance DNA break survival. However, GreB overexpression can substitute for GreA in promoting DSB sensitivity (Extended Data Fig. 2b and Supplementary Discussion).

DksA is a transcription initiation<sup>12</sup> and elongation factor<sup>13</sup> that also interacts with the RNAP secondary channel. DksA does not perform transcript cleavage, but competes with the Gre

factors for RNAP binding<sup>14</sup>. In the absence of DksA, viability was reduced compared with wild-type cells upon phleomycin treatment (Figs. 1a,b). The phleomycin sensitivity of *dksA* cells was largely suppressed by removal of GreA (Figs. 1a,b). Moreover, overexpression of DksA enhanced the phleomycin resistance of wild-type cells (Fig. 1c), suggesting that exclusion of GreA from RNAP by competition with DksA increases survival after DSB induction. The lower phleomycin resistance of the *dksA greA* double mutant compared with the *greA* mutant was unchanged even in the absence of GreB (Fig. 1d), suggesting that, in addition to competing with Gre, DksA alone may promote DSBs repair.

We next used pulsed-field gel electrophoresis (PFGE) to visualize the kinetics of repair after DNA breakage (Fig. 1e). In the *dksA* mutant, phleomycin treatment resulted in extensive chromosome fragmentation (Figs. 1f,g). After phleomycin removal, DNA fragmentation levels gradually declined, indicating slow DNA repair (Figs. 1f,g). In contrast, *dksA greA* cells exhibited much faster repair of fragmented DNA and showed higher survival than *dksA* cells (Figs. 1f,g and Extended Data Figs. 3a,b). The accelerated repair in the absence of GreA was abrogated by inactivation of the RecA recombinase (Figs. 1f,g). Without *recA*, break repair deficiency caused persistent DNA fragmentation (Extended Data Figs. 3c,e). Enhanced DNA repair was also observed in the *greA* single mutant compared with wild-type cells, albeit at a less pronounced level (Extended Data Fig. 3d), possibly due to the contribution of DksA to DSB repair. In agreement with the PFGE results, the increased survival of the *greA* mutant after phleomycin treatment was almost completely dependent on RecA (Fig. 1h). These data indicate that GreA impedes DSB repair via the canonical RecA-dependent homologous recombination pathway.

To confirm that the phleomycin resistance of *greA* cells was specific to the repair of DSBs, we used an inducible DNA break system consisting of the I-SceI endonuclease<sup>15</sup> along with I-SceI recognition sites engineered at various chromosomal loci (Fig. 2a). Induction of I-SceI resulted in ~100-fold killing in wild-type cells (Fig. 2b). Deletion of *greA* increased survival upon I-SceI break induction by ~10-fold (Fig. 2b), indicating enhanced repair of a single DSB using sister homology in the absence of GreA. Survival of the *dksA* mutant was reduced compared with wild-type cells (Fig. 2b), while deletion of *greA* restored viability to the level of wild-type but not to that of the *greA* mutant (Fig. 2b), implying again that DksA may independently promote DSB repair. The increased viability after I-SceI induced DSBs in the *greA* mutant required *recA* and *recB* (Fig. 2c). Elimination of RecD, which abolishes 5'-3' helicase and RecB nuclease activities but increases homologous recombination proficiency<sup>2,16</sup>, did not affect the DSB resistance of *greA* mutants (Fig. 2c and Extended Data Fig. 4a). Thus, RecB (Figs. 1h and 2c) but not RecD functions are involved in the repair phenotype of the *greA* mutant. Additionally, the GreA effect on break repair did not require the RecJ exonuclease or the RecA loading RecFOR complex, which function in a secondary pathway of recombination<sup>2,17</sup> (Extended Data Figs. 4b-d and Supplementary Discussion).

The influence of GreA on I-SceI DSB survival was not locus-specific as we obtained similar results at the *yjaZ* site (Figs. 2a,b). Both the *yjaZ* and *lac* loci are located in highly transcribed regions. In contrast, deletion of *greA* produced no survival advantage over wild-type cells when the I-SceI site was engineered within the lambda prophage, a predominantly

transcriptionally silent region<sup>18</sup> (Extended Data Figs. 4e,f), suggesting that transcription is required in areas surrounding the break site to promote DSB resistance in absence of GreA.

## Backtracked RNAP increases DSB repair

To understand how the absence of GreA promotes break repair, we first determined that the DNA damage response (Extended Data Figs. 4g–i) and R-loop formation (Extended Data Fig. 5a) were not involved in the DSB resistance of *greA* mutants (Supplementary Discussion). Next, we tested if the phleomycin resistance of *greA* mutants was dependent on known factors that control RNAP backtracking. Deletion of *mfd*, a TCR-dependent helicase that reactivates backtracked RNAP by pushing it forward<sup>6</sup>, produced no significant change in the phleomycin resistance of the *greA* mutant (Fig. 2d). Removal of UvrD, which opposes GreAB action by pulling RNAP backwards in the secondary TCR pathway<sup>7</sup>, reduced the phleomycin resistance of *greA* cells (Fig. 2d), implying a function for UvrD in promoting DSB repair in absence of GreA. This role is likely independent from the mismatch repair and nucleotide excision repair functions of UvrD<sup>19</sup> (Extended Data Fig. 5c). The small molecule ppGpp acts in concert with UvrD to promote RNAP backtracking and facilitate TCR<sup>20</sup>. Cells lacking ppGpp are sensitive to phleomycin, whereas overproduction of ppGpp by the *spoT203* allele rendered cells resistant to DSBs with the help of UvrD (Extended Data Fig. 5b). Thus, as in the TCR pathway<sup>20</sup>, the combined action of UvrD and ppGpp on RNAP backtracking may also stimulate DSB repair. ppGpp along with DksA also regulates the stringent response through binding to RNAP<sup>21</sup>. We examined the phleomycin phenotype of RNAP mutations that disrupt ppGpp-RNAP interactions<sup>22,23</sup> and found that the site 2 mutant, which abolishes the stringent response behaved like wild-type cells (Extended Data Fig. 5b), suggesting that stringent response activation by ppGpp and DksA was not required for phleomycin resistance. The site 1 mutant and ppGpp null cells were equally sensitive to phleomycin (Extended Data Fig. 5b), suggesting that this site could be involved in DNA break repair.

We also examined the phleomycin survival phenotypes of RNAP mutants that are more or less susceptible to backtracking and found that accumulation of UvrD-dependent backtracked RNAP results in DNA break resistance (Extended Data Figs. 5b,d,e and Supplementary Discussion).

## XO-Seq captures features of DSB repair

To determine at what stage GreA inhibits DSB repair, we developed an assay to analyze the different steps of DSB repair in living cells. Our method combined massive parallel sequencing with I-SceI DSB induction (XO-Seq, eXOnuclease Sequencing) to generate a genome-wide landscape of DNA loss from exonucleolytic resection of break ends during repair (Figs. 3a,b). In wild-type cells, XO-Seq read counts revealed a decrease in DNA content around the break site (Fig. 3b and Extended Data Fig. 6a), which far exceeded the boundaries of many transcription units (Extended Data Fig. 6e). Read counts reached a steady state after 30 min, reflecting a balance between I-SceI cutting, resection and repair synthesis (Fig. 3b). However, read loss was asymmetrical around the break site, extending less than 100 kb in the origin (*oriC*)-proximal side, but more than 200 kb in the origin-distal

direction (Fig. 3b and Extended Data Fig. 6f). This skewing can be mainly attributed to the disproportionate number of active Chi sites upstream of the break and can be switched by inverting a portion of the chromosome (Extended Data Figs. 7a,b), validating the broken fork repair model<sup>24</sup> (Supplementary Discussion).

The pattern of sequencing reads around the break site provides a way of analyzing resection and recombination activity (Supplementary Methods). The experimental curves were reproduced using a mathematical model, which describes the stochastic process of RecBCD-dependent DNA resection (Fig. 3c, Extended Data Fig. 7d and Supplementary Methods). Furthermore, the model parameters used in fitting the experimental data inform us about key physiological parameters: RecBCD processivity and Chi site sensitivity (Extended Data Fig. 7c).

We validated that DNA attrition in the vicinity of the DSB represents recombination processes by analyzing the behavior of *recD* mutants that showed reduced DNA degradation (Fig. 3d and Extended Data Fig. 6b) and *recA* mutants that displayed massive degradation (Fig. 3e and Extended Data Figs. 6c, 7e) and conclude that XO-Seq captures known features of break repair (Supplementary Discussion).

## RNAP backtracking reduces RecBCD resection

Next, we used XO-Seq to evaluate how GreA inhibits DSB repair. Read counts in *greA* cells also reached a steady state. But, at 30 and 60 min after DSB induction, *greA* cells had significantly more reads around the break site compared with wild-type cells (Figs. 4a,b), which could reflect either reduced resection or increased repair synthesis following recombination. To differentiate between these possibilities, we first tested resection dynamics in the repair impaired *recA greA* mutant. *recA greA* cells displayed slightly less degradation than the *recA* single mutant (Extended Data Fig. 7f), suggesting that GreA promotes resection to some extent even in the absence of RecA. To alleviate the analytical complications of massive chromosome loss in the *recA* mutant, we used a thermosensitive allele of DNA polymerase III (*dnaEts*), which abolishes repair synthesis when inactivated<sup>25</sup> (Extended Data Figs. 1a, 6d, 8a). At the restrictive temperature, we observed significantly less resection in the *dnaEts greA* mutant compared with the *dnaEts* single mutant (Fig. 4c). Thus resection and not repair synthesis is reduced in the absence of GreA. Moreover, removal of *greA* produced no degradation change in the exonuclease mutants *recB* (Fig. 4d) or *recB recJ* (Extended Data Figs. 8b–d), indicating that GreA impedes RecB-dependent resection (Supplementary Discussion).

The reduced DNA resection in the absence of GreA suggests that the accumulation of backtracked RNAP on DNA may slow RecBCD processing. Thus, inhibition of transcription should increase DNA resection. Treatment of wild-type cells with the transcription inhibitor rifampicin increased DNA resection (Fig. 5a), independent of the DNA damage response (Fig. 5b, Extended Data Figs. 8e–g and Supplementary Discussion). Furthermore, the reduced resection observed in the *greA* mutant compared to wild-type cells disappeared in the presence of rifampicin, suggesting that the GreA effect on resection required transcription (Fig. 5c). To study the influence of transcription on RecBCD resection with

reduced Chi site interference, we created a strain with no Chi sites for 122 kb downstream of the DSB site. DNA degradation within the Chi-free region was increased compared with the strain containing natural Chi sites (Extended Data Fig. 9a). DNA degradation and I-SceI DSB survival in the Chi-free strain correlated with RNAP backtracking levels (Extended Data Figs. 9b, c). As transcription is required to produce backtracked RNAP, these results support the hypothesis that the accumulation of backtracked RNAP due to the lack of GreA to restart transcription restricts resection and promotes DSB repair.

### ***greA* restores RecA loading deficiency**

A key function of RecBCD is to direct RecA nucleation onto ssDNA at Chi sites<sup>4</sup>. Inactivation of *recD* causes early and Chi-independent RecA loading<sup>26</sup> resulting in reduced DNA degradation (Fig. 3d), which is further reduced in the *recD greA* double mutant (Extended Data Fig. 9d), implying that both of these proteins independently but similarly reduce resection. Deletion of *recD* suppresses the recombination and damage-survival phenotypes of the *recB* D1080A point mutant (*recB\**), which lacks nuclease and Chi-dependent RecA loading activities<sup>16,27</sup>. *recB\** cells have restricted repair function due to the partial substitution of exonuclease activity by RecJ and the RecFOR complex assisting in RecA filament formation<sup>28</sup> (Extended Data Fig. 9e). Deletion of *greA* increased the phleomycin resistance of *recB\** mutants and the *recB\* recF greA* strain also showed a significant phleomycin survival advantage compared with the *recB\* recF* mutant (Fig. 5d). However, both the *recB\* recJ* and *recB\* recJ greA* mutants displayed poor viability even in the absence of DNA damage (Extended Data Figs. 9 f,g). This separation-of-function experiment suggests that whereas removing GreA can suppress the inability of *recB\* recF* mutants to load RecA, RecJ exonuclease activity is required for DSB repair in the *recB\* greA* mutant. Thus, enhanced repair in the *greA* mutant requires the helicase and nuclease activities of resection, but can bypass the Chi-dependent RecA loading function required for repair, suggesting that the absence of GreA can promote RecA loading independent of Chi sites.

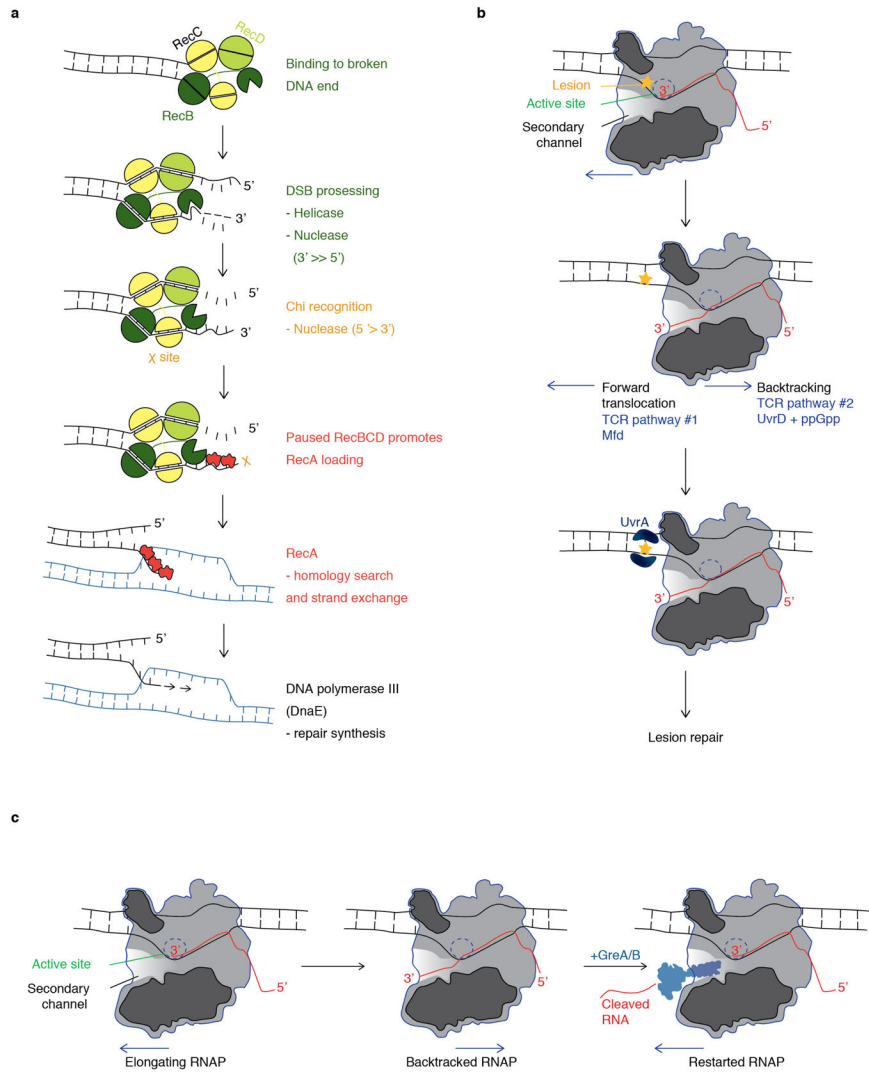
### **Transcription fidelity impedes DSB repair**

Our results show that increasing backtracked RNAP promotes DSB repair by the RecBCD-RecA pathway. We found that the build-up of backtracked RNAP that occurs in the absence of GreA reduces RecBCD resection, as well as the requirement for specific RecA loading activity of RecB. We propose that backtracked RNAPs can instigate recombination in a manner similar to Chi sites (Fig. 5e). Backtracked RNAPs that can form stable complexes on DNA<sup>9</sup> could provoke RecBCD pausing<sup>5</sup>, which in turn can stimulate RecA loading<sup>29</sup> and enhance DSB repair. Interestingly, in eukaryotes, mutations in the THO/TREX transcription elongation complex result in phenotypes similar to the *greA* mutant including hyper-recombination<sup>30</sup>, which maybe in part due to increased backtracked RNAP.

Our finding that DSB repair becomes more efficient when transcription processivity is compromised suggests a trade-off between the completion of transcription elongation, which maintains transcription fidelity, and preservation of genome stability by repairing DNA. The role of RNAP backtracking in promoting transcription fidelity and suppressing repair

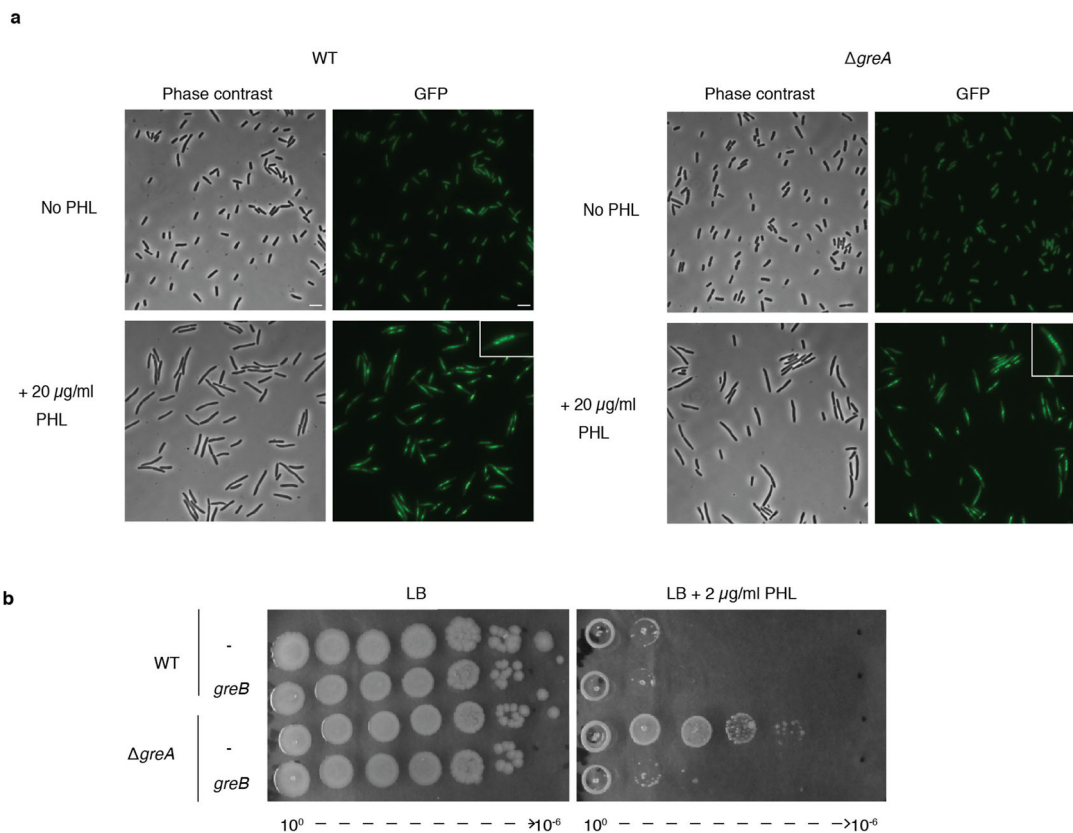
highlights the importance of GreA function. GreA is conserved across bacterial species and the eukaryotic homolog of GreA, TFIIS, is also a transcript cleavage and fidelity factor<sup>31</sup>. Intriguingly, the synthesized minimal living bacterial genome requires GreA, whereas RecA was found to be dispensable<sup>32</sup>. The consequences of RNA errors in epigenetic inheritance<sup>33</sup> and proteome toxicity<sup>34</sup> are being explored as a mechanism underlying evolution and disease. In the radiation resistant bacterium *Deinococcus radiodurans*, tolerance to DNA breaks mostly depends on a robust proteome for proper DNA repair and not on more efficient DNA repair<sup>35</sup>. The protection of the proteome afforded by high fidelity transcripts could be one plausible explanation for why transcription fidelity is favored over fixing broken chromosomes, which can be more easily replaced using sister homologies present during active growth. This highlights a possible evolutionary equilibrium between RNA and DNA integrity that remains to be understood.

### Extended Data



### Extended Data Figure 1. DSB repair by the RecBCD-RecA pathway, TCR and RNAP backtracking

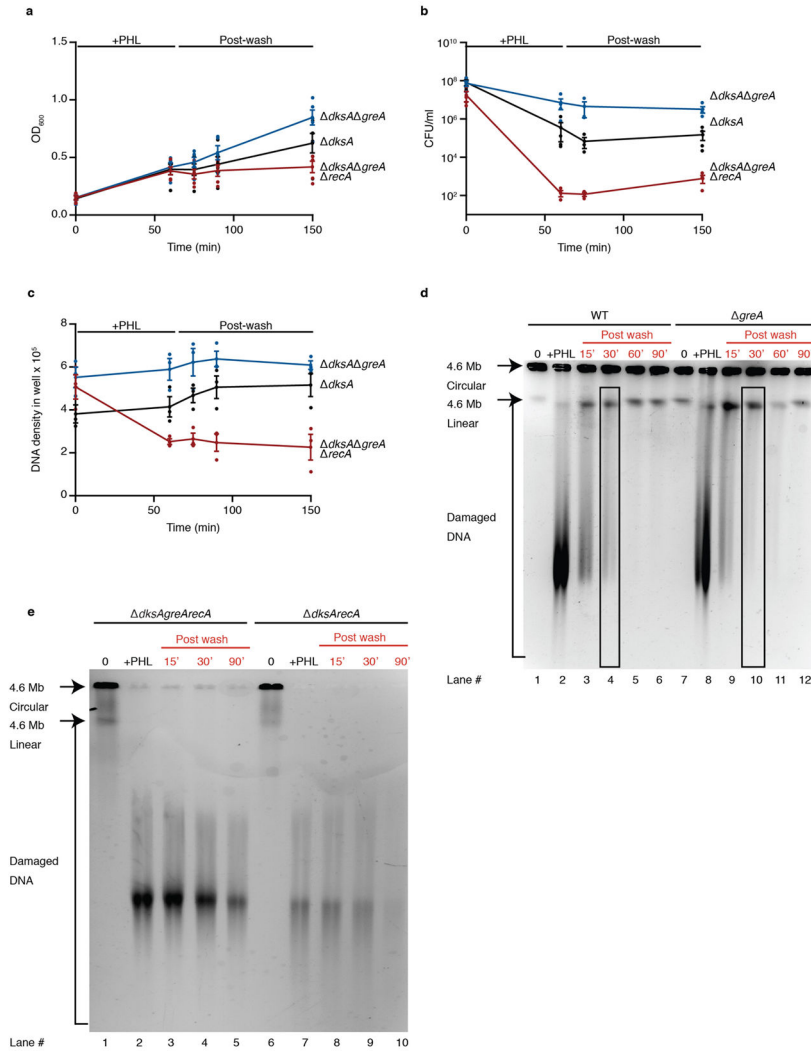
a, The RecBCD tri-subunit complex binds to blunt DSB ends with high affinity. The enzyme uses translocase, helicase and nuclease activities to move along the DNA while unwinding and degrading the DNA. RecB is a helicase with 3' → 5' translocation polarity, whereas RecD acts on the other strand<sup>2</sup>. Initially, the 3' end of DNA is degraded more vigorously than the 5' end<sup>3</sup>. When RecBCD encounters an 8bp Chi site that is recognized by the RecC subunit<sup>36</sup>, the nuclease polarity is switched and unwinding proceeds at a slower rate resulting in the formation of ssDNA overhangs onto which RecA is loaded. The RecA-ssDNA filament performs the homology search and invades the homology donor (blue). DNA from the donor is copied by DNA polymerase III (DnaE). b, Transcription-coupled DNA repair (TCR) is initiated when RNAP is stalled at a bulky or helix-distorting lesion. UvrD and ppGpp together can pull RNAP backwards<sup>20</sup>, or alternatively Mfd can promote RNAP forward translocation<sup>6</sup>. Either of these processes expose the DNA lesion, allowing it to be accessed and repaired by UvrA (blue) and other proteins (not shown) in the nucleotide excision repair pathway (NER)<sup>19</sup>. c, Elongating RNAP can undergo reverse translocation or backtracking along the DNA template. When this happens, the 3' end of the nascent transcript, which was originally within the active site of RNAP, gets extruded into the secondary channel. Hence, transcription elongation cannot continue<sup>9</sup>. GreA and GreB can independently stimulate the internal hydrolytic cleavage of the RNA, realigning the 3' end within the active site of RNAP, allowing for the restart of transcription elongation<sup>9,10</sup>.





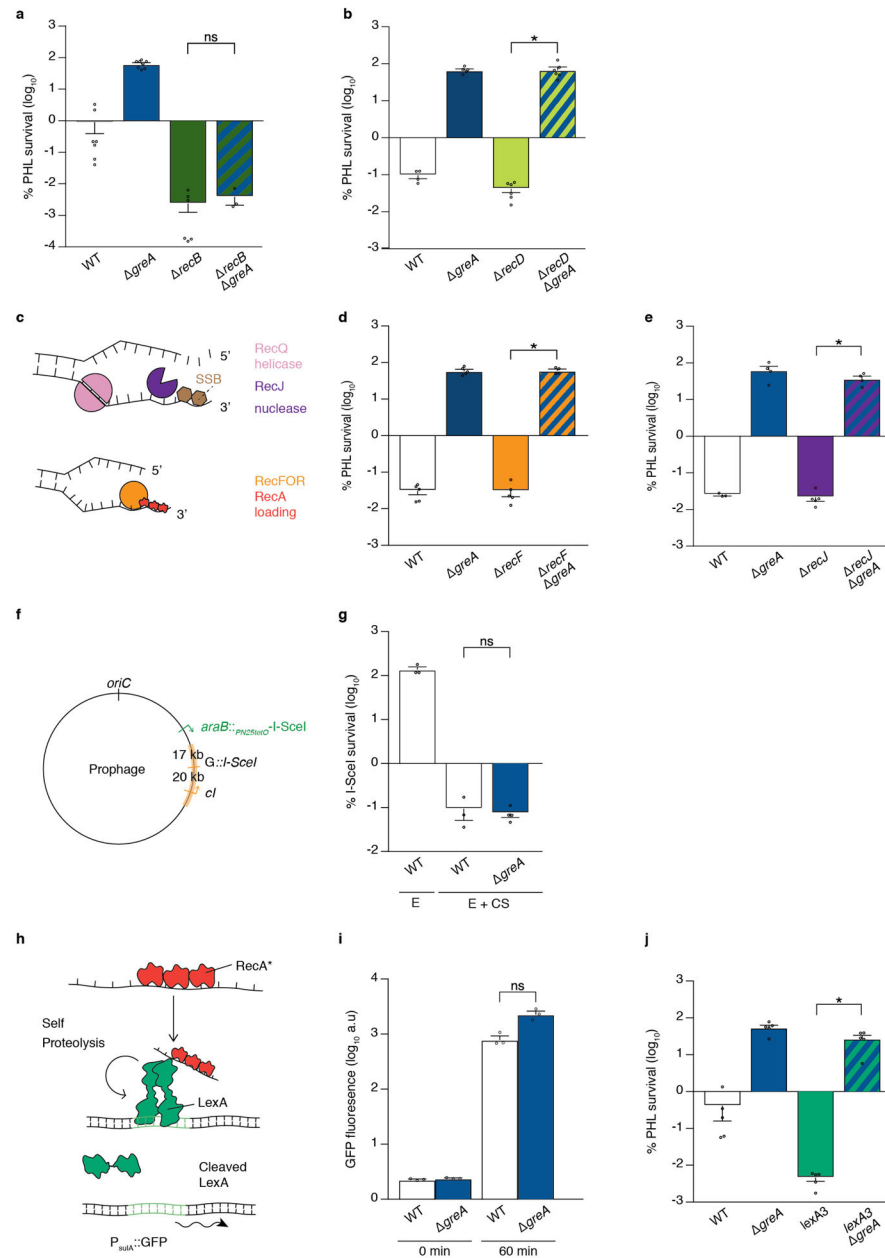
**Extended Data Figure 2. DSB generation and PHL phenotype of GreB overexpression**

a, DSB formation is unaffected by removal of *greA*. Mu GamGFP (Gam protein from phage Mu fused to GFP<sup>37</sup>) foci formation in wild-type (WT) and *greA* cells after treatment with 20 µg/ml phleomycin (PHL) compared to untreated (No PHL). Enlarged cells are shown in the upper right corner. Without treatment, 3 to 5 % of WT and *greA* cells have only one GamGFP focus. After PHL treatment, 87% of WT cells and 77% of *greA* cells have multiple GamGFP foci. b, GreB, when present at the appropriate levels can also modulate PHL sensitivity. Representative (1/3) semi-quantitative spot assay of 10-fold serially diluted log phase cultures from strains overexpressing GreB from its native promoter on a high copy plasmid at the indicated PHL concentrations. GreB overexpression, but not the pBA169 plasmid only control (-), suppresses the PHL resistance of the *greA* deletion.

**Extended Data Figure 3. Pulsed-field gel electrophoresis analysis**

a,b, OD<sub>600</sub> (a) and survival (b) measured at each of the time points at which samples were obtained for pulsed-field gel electrophoresis (PFGE) in the *dksA*, *dksA greA* and *dksA recA greA* mutants, described in Fig. 1f and 1g. c, Intensity of DNA within the

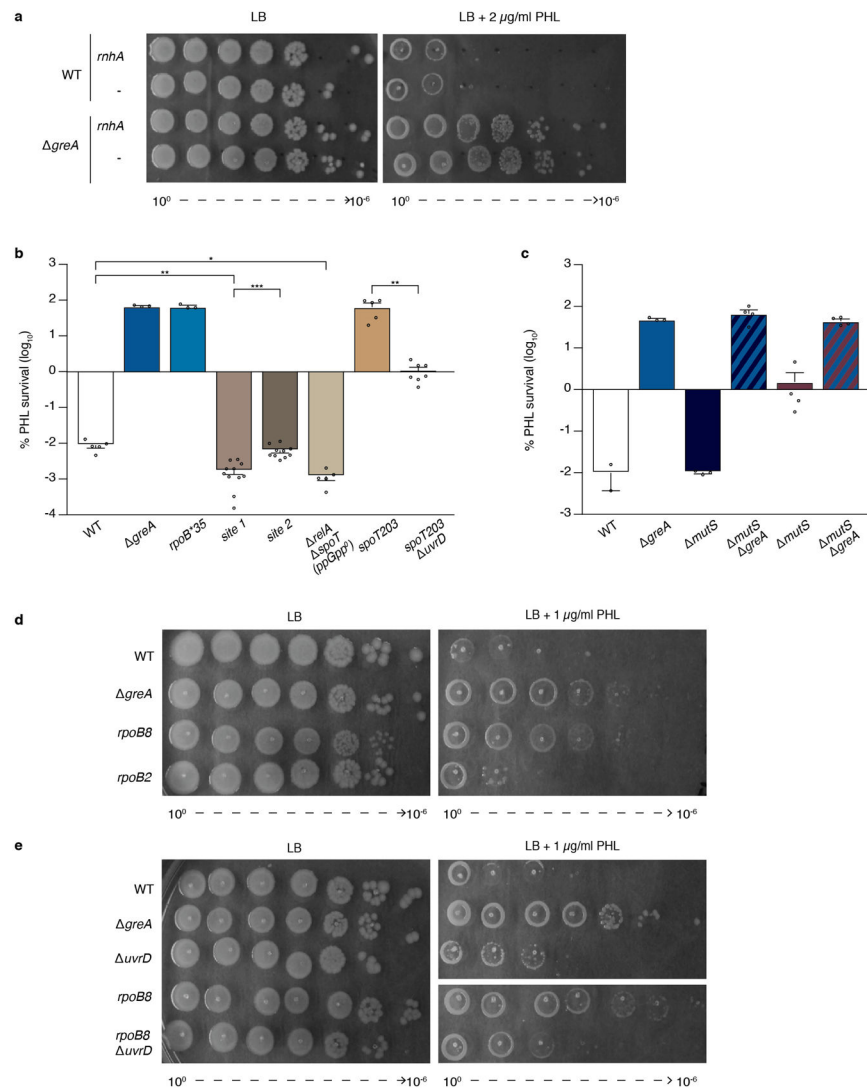
well, which is composed of intact circular *E. coli* genomes, as determined by densitometric analysis. For a–c, n = 3 biological replicates (cultures), data are mean ± s.e.m. d, Representative PFGE of wild-type (WT) and *greA* strains before (lanes 1,7), after 60 min of treatment with 20 µg/ml phleomycin (PHL) (lanes 2,8) and at indicated times after washing out the drug (lanes 3–6, 9–12). Black bars highlight the observable DNA fragmentation difference between *greA* and WT cells at 30 min after removing PHL. e, Representative PFGE of the *dksA recA greA* and *dksA recA* mutants after treatment with 20 µg/ml PHL (lanes 2,7) and at indicated times after washing out the drug (lanes 3–5, 8–10), showing that unrepaired fragmented DNA is eventually degraded in *recA* mutants both in the presence and absence of GreA. For source data see Supplementary Figure 1.



#### Extended Data Figure 4. Factors influencing DSB resistance in the *greA* mutant

a, Deletion of *recD* does not alter the PHL resistance of *greA* cells (1  $\mu$ g/ml PHL). b, In the absence of RecBCD, an alternate repair mode involving the RecQ helicase, RecJ exonuclease and RecF assisted RecA-ssDNA filament formation (by displacing SSB) can repair DSBs<sup>2,17,38</sup>. c, RecF is not required for the PHL (1.5  $\mu$ g/ml) resistance of *greA* strains. d, RecJ is also not required for the PHL (1  $\mu$ g/ml) resistance of *greA* strains. e, Schematic representation of the I-SceI cutsite engineered within the phage lambda genome (prophage). The I-SceI enzyme is expressed from the doxycycline-induced *P<sub>N25-tetO</sub>* promoter. f, Generation of a DSB in the prophage genome reduces the survival of wild-type (WT) and *greA* cells equally. g, The DNA damage (SOS) response is activated when RecA

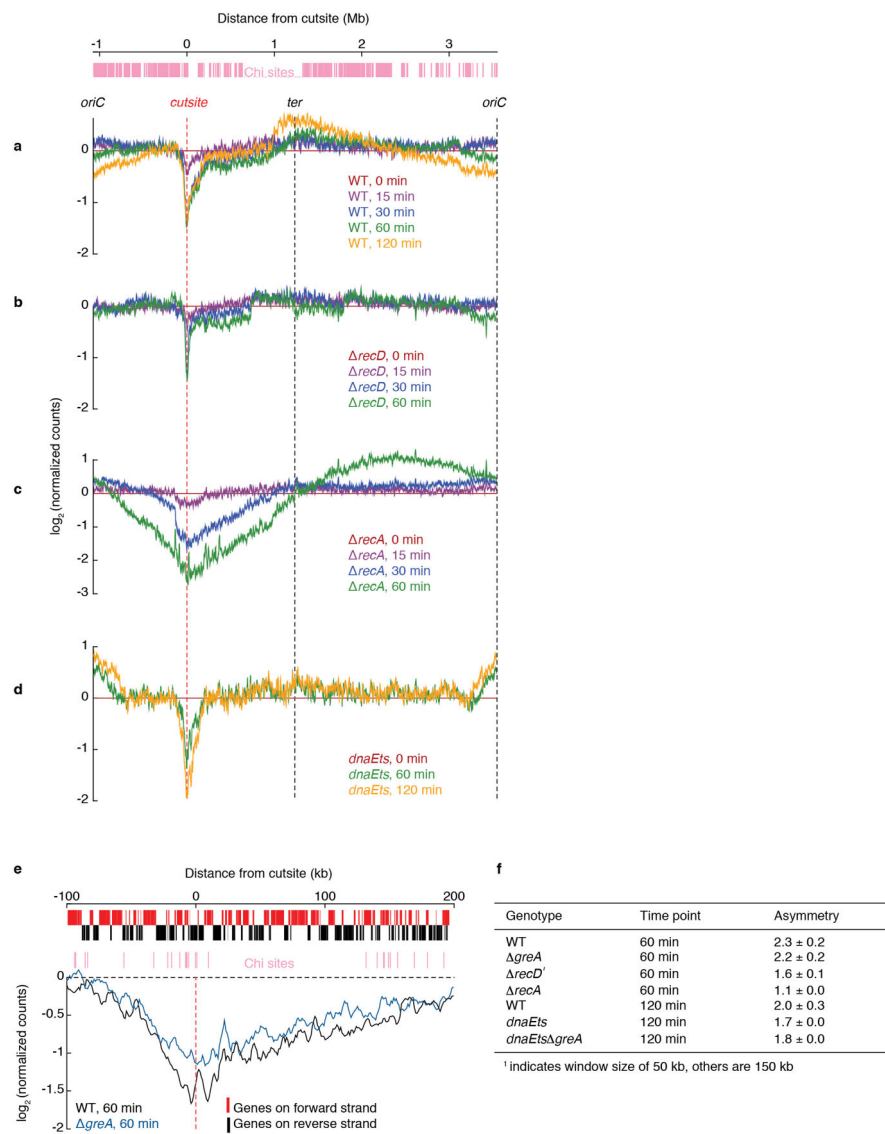
bound to single stranded DNA (RecA\*) stimulates the self-proteolytic cleavage of the transcriptional repressor LexA, which is part of the SOS regulon. The SOS response can be monitored using a transcriptional fusion of the promoter of *sulA* to GFP<sup>39</sup>. h, Flow cytometry analysis of P<sub>*sulA*</sub>-GFP expression shows no significant difference between WT and *greA* cells, before (0 min) and 60 min after I-SceI DSB induction at the *lacA* locus. Gating was performed using the *lexA3* allele, n = 3, data are mean ± s.e.m; p = 0.05 (Mann-Whitney U test). i, PHL resistance of the *greA* mutant is unaffected by the inability of cells to activate the SOS response using the *lexA3* allele (PHL used at 1 µg/ml). For a–c, e,f,h and k, n = 3 biological replicates (cultures), mean ± s.e.m; p = 0.01 (\*\*); p = 0.05 (\*); p = 0.05 (ns) (Kruskal-Wallis test with multiple testing correction).



### Extended Data Figure 5. Pathways of RNAP backtracking and their influence on phleomycin resistance

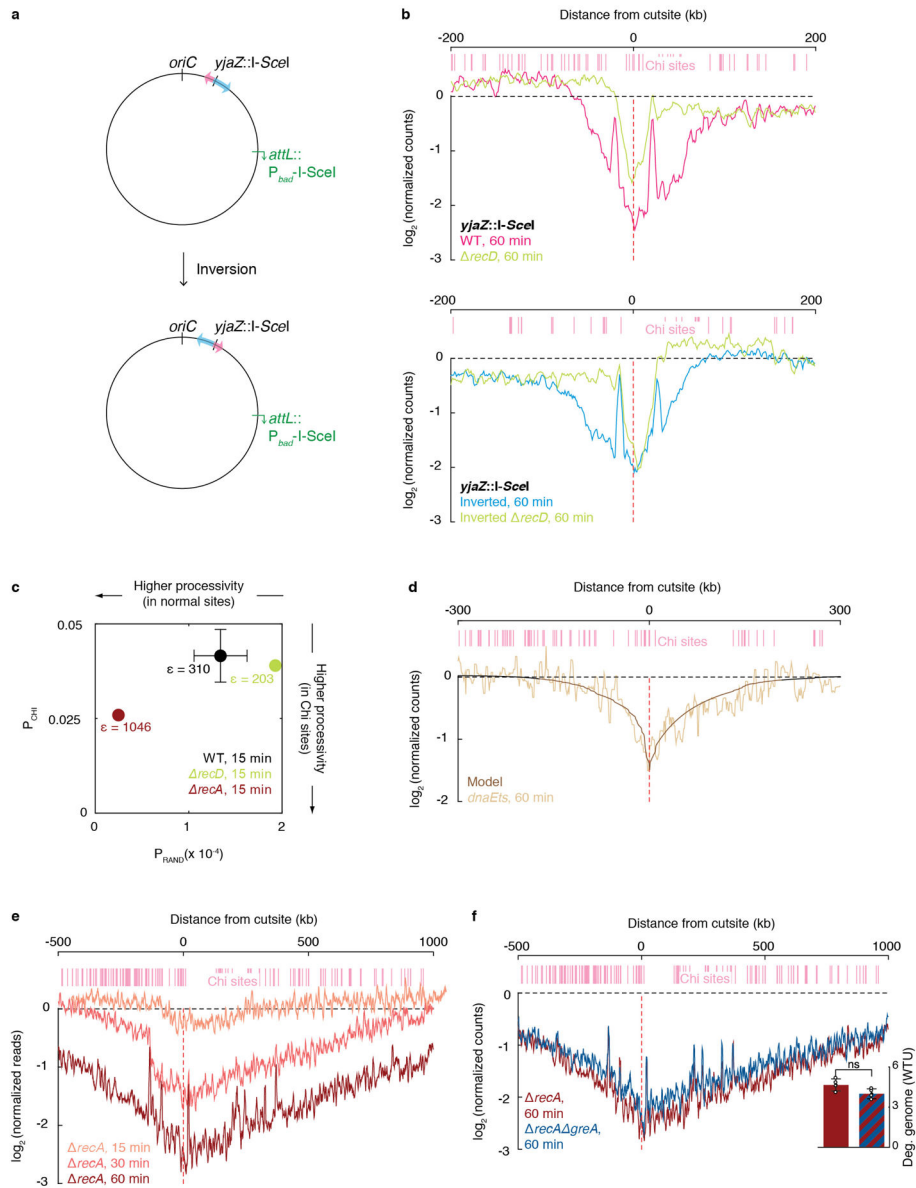
a, Overexpression of RnaseH does not affect the phleomycin (PHL) phenotype of wild-type (WT) or *greA* mutants; RnaseH plasmid (pSK760 *rnhA*) and control plasmid (pSK762 –)

(1/3 representative biological replicates, cultures). Plasmid pSK760 was confirmed as RnaseH overexpressing by transforming into a *dnaAts rnhA* mutant, growth of which would be rescued only if the plasmid expressed wild-type *rnhA*<sup>40</sup>. b, PHL survival phenotypes of the indicated mutants at 1.5 µg/ml PHL, n = 3 biological replicates (cultures), mean ± s.e.m;  $p < 0.001$  (\*\*\*),  $p < 0.01$  (\*\*),  $p < 0.05$  (\*) (Kruskal-Wallis test with multiple testing correction). c, Resistance of *greA* mutants to 1.5 µg/ml PHL is not affected by deletion of *uvrA* (NER) or *mutS* (mismatch repair), n = 2 biological replicates (cultures), mean ± s.e.m. d, e, Representative (1/3) semi-quantitative spot assay of cultures grown to OD<sub>600</sub> = ~0.4 in LB, 10-fold serially diluted, and plated on LB agar at the indicated PHL concentrations. *rpoB8*, a slow transcribing RNAP mutant prone to backtracking<sup>41</sup> is resistant to PHL while *rpoB2*, a mutation that makes RNAP elongate faster<sup>42</sup> is sensitive (d). PHL resistance of *rpoB8* is suppressed by deletion of *uvrD* (e).



**Extended Data Figure 6. Genome levels effects of XO-Seq**

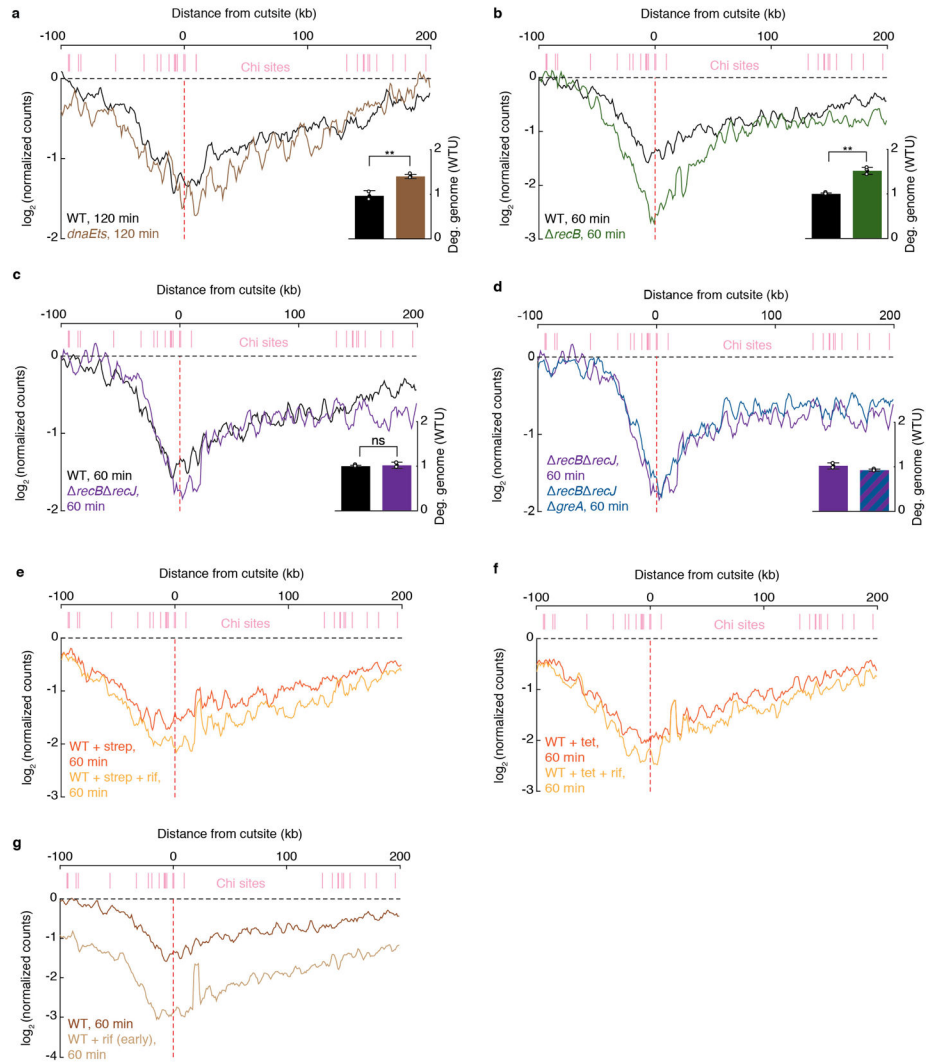
a, Normalized read counts of wild-type (WT) cells across the 4.6 Mb *E. coli* genome at the indicated times after I-SceI DSB generation at *lacA*. Read loss is restricted to regions on either side of the break site. However, DNA content changes at *oriC* and *ter* can be seen due to normalization of each time point relative to the un-induced (0 min) sample. DNA degradation seen around the break site is greater than previously reported for *in vivo* DSB generation at *lacA*<sup>43</sup>. This discrepancy could arise from the Tagmentation procedure (Illumina®) used to fragment and tag DNA that captures only double-stranded DNA and may miss single-stranded DNA substrates formed after Chi recognition, or from the differences in the reparability of the two systems. b, c, Normalized read counts of *recA* and *recD* mutants across the genome at the indicated times after I-SceI induction at *lacA*, showing reduced DNA degradation in the absence of RecD (b), but extensive ‘Rec-less’<sup>44</sup> DNA loss without RecA (c). d, Whole genome reads from the *dnaEts* mutant at the indicated times showing read pattern changes at *oriC* (higher copy number than WT) and *ter* (lower copy number than WT) consistent with the inactivation of replication by DNA polymerase III (*dnaE*)<sup>25</sup>. e, Position and orientation of transcribed genes around the *lacA*::I-SceI cutsite. f, Quantification of asymmetry in the indicated strains and times after DSB induction. Window size is  $\pm 150$  kb for all strains and times except for *recD* where window size  $\pm 50$  kb.



### Extended Data Figure 7. Chi asymmetry effects, mathematical modeling and extensive DNA degradation identified by XO-Seq

a, Location of 920 kb inversion that surrounds the *yjaZ*::I-SceI outsite, but does not include *oriC*. b, Representative curves (1/2 biological replicates) of sequencing in wild-type (WT) and *recD* strains compared to strains after inversion of part of the genome (WT and *recD*), 60 min after DSB generation at *yjaZ*. c, Parameters of the mathematical model of RecBCD resection obtained from fitting the degradation curves at 15 min for WT, *recD* and *recA* mutants. Also shown are the Chi sensitivities ( $\epsilon$ ) from each fit,  $n = 2$  biological replicates (cultures), data are mean  $\pm$  s.d. d, The mathematical model of RecBCD resection fits well with the degradation curve obtained 60 min after I-SceI break induction at *lacA* in the *dnaEts* background. e, Representative (1/4) plot of read patterns obtained after I-SceI break induction at *lacA* in the *recA* mutant at the indicated time points. f, XO-Seq plots

comparing *recA* and *recA greA* mutants, representative (1/4) plot shown, inset bar plot is from n = 4 biological replicates (cultures), data are mean  $\pm$  s.d, Deg. DNA (WTU) is genome degradation relative to WT in wild-type units.

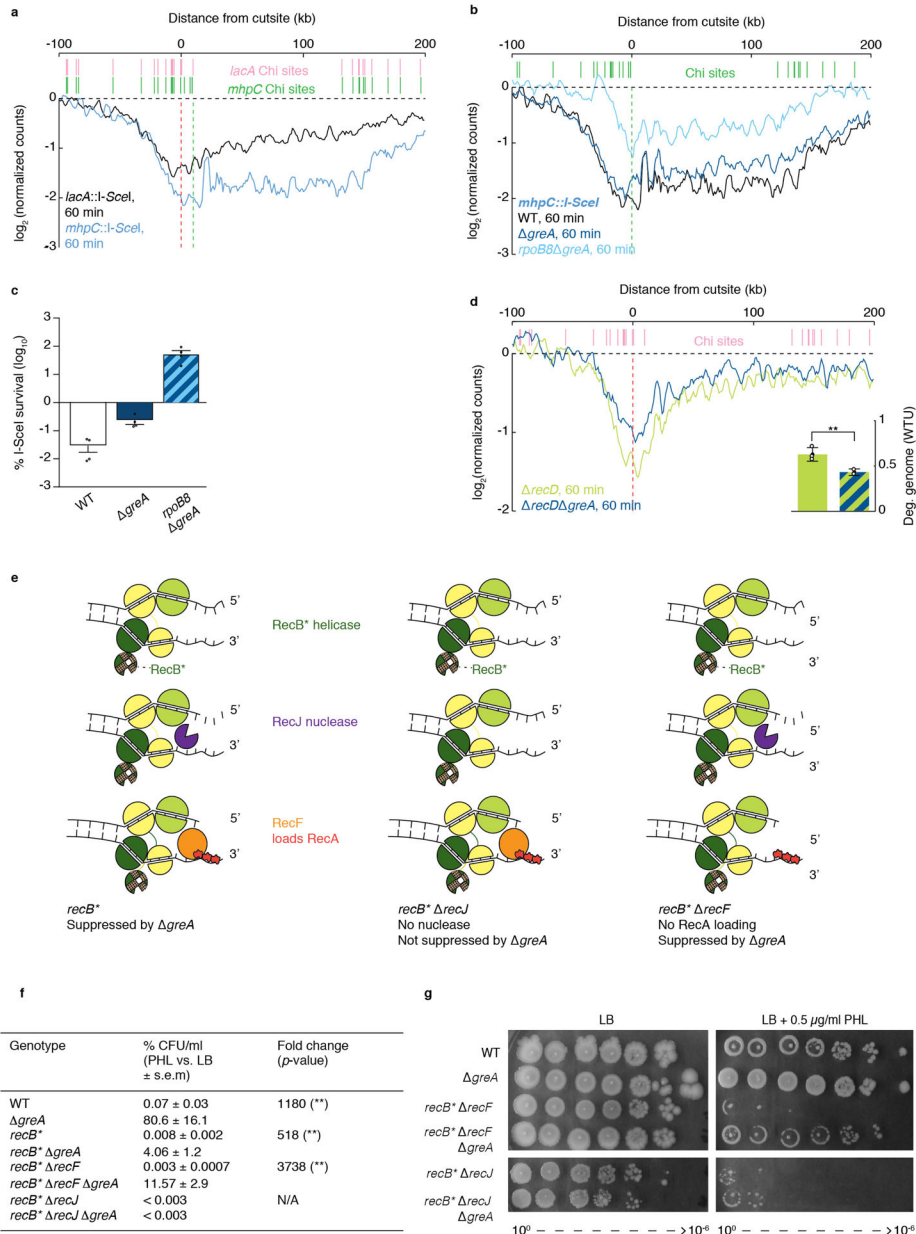


### Extended Data Figure 8. Resection and DNA damage response influence on XO-Seq read patterns

a, Read patterns in wild-type (WT) and the *dnaEts* mutant 120 min after I-SceI induction at *lacA* and temperature shift to 42°C to inactivate *dnaE*<sup>25</sup>, showing that *dnaE* function is removed at 120 min. b, Read count patterns in WT and *recB* showing greater DNA degradation in the absence of *recB*. c, Degradation is reduced in the *recB recJ* background, suggesting that RecJ contributes to resection when RecB is not present. d, Degradation is similar in *recB recJ* and *recB recJ greA* cells. For a–d representative plots shown after inducing I-SceI DSB at *lacA* for the indicated times, the inset bar plots are from n = 2 biological replicates (cultures), data are mean  $\pm$  s.d,  $p < 0.01$  (\*\*),  $p < 0.05$  (ns) (Two-tailed two sample *t*-test); Deg. DNA (WTU) is genome degradation relative to WT in wild-type units. e, f Read count patterns in WT after treatment with streptomycin (strep)



compared to treatment with strep and rif (e) and WT after treatment with tetracycline (tet) compared to treatment with tet and rif (f). g, WT after treatment with rif, 15 min after I-SceI induction.



**Extended Data Figure 9. Effect of RNAP backtracking on DSB repair in a ‘Chi free’ region and mechanism of reduced resection in *greA* mutants**

a, Comparison of read count patterns after 60 min of DSB induction at the *lacA* and *mhpC* loci. Vertical red and green lines show positions of the I-SceI recognition site at *lacA* and *mhpC* respectively, and the pink and green bars show the positions of correctly oriented Chi sites for *lacA* and *mhpC* respectively. b, Read count patterns 60 min after DSB induction at *mhpC* in wild-type (WT) compared with *greA*, and *rpoB8 greA* mutants, where increasing

backtracked RNAP complexes are formed. c, The *rpoB8 greA* mutant shows an increased effect on survival after DSB induction at *mhpC* compared with *greA* and WT cells; n = 4 biological replicates (cultures), data are mean  $\pm$  s.e.m. d, The *recD greA* mutant has reduced degradation compared with the *recD* mutant alone 60 min after DSB induction at *lacA*, representative plot show, inset bar plot is from n = 2 biological replicates (cultures), data are mean  $\pm$  s.d,  $p < 0.01$  (\*\*) (Two-tailed two sample *t*-test); Deg. DNA (WTU) is genome degradation relative to WT in wild-type units. e, Substitution of aspartic acid with alanine at position 1080 in the nuclease domain of *recB* (*recBD1080A* or *recB\**) abolishes the ability of RecB to perform nuclease and RecA loading activities<sup>16,27,28</sup>. RecJ can compensate for the nuclease function and RecF aids in RecA filament formation, resulting in a hybrid resection machine composed of RecB helicase, RecJ exonuclease and RecF assisted RecA loading<sup>28,45</sup>. Suppression of each individual function by the *greA* mutant is indicated. f, Phleomycin (PHL) survival of the indicated mutants as graphed in Fig. 5d. The *recB\* recJ* and *recB\* recJ greA* mutants produced no countable colonies on PHL; n = 3 biological replicates (cultures), data are mean  $\pm$  s.e.m,  $p < 0.01$  (\*\*) (Kruskal-Wallis Test with multiple testing correction). g, Representative (1/4) semi-qualitative spot assay showing that the *greA* deletion can suppress the PHL sensitivity of the *recB\* recJ* mutant but not the *recB\* recJ* mutant at a low concentration of PHL (0.5  $\mu$ g/ml).

**a**

Plasmid	Features	Reference <sup>1</sup>
pKD3	FRT <i>cam</i> FRT	46
pKD4	FRT <i>kan</i> FRT	46
pcp20	flp+ $\lambda$ <i>cl857</i> $\lambda$ pR repts <i>ampR camR</i>	47
pBR322	<i>ampR</i>	
pBR322-DksA	<i>ampR</i>	48
pBA169	<i>ampR</i>	
pBA169-GreB	<i>ampR</i>	48
pSK760-RnhA	<i>ampR</i>	41
psK763-c	<i>ampR</i>	41
pUA66-	<i>psuA::gfpmut2-</i>	49
psuA::gfpmut2	<i>kanR</i>	
pTSA29-CXI	<i>cl857-PR-(<math>\lambda</math>xis-<math>\lambda</math>int)</i>	50

<sup>1</sup> See supplementary references

**b**

Primer	Sequence
OC 170	5' gcgccattccgaccaacatatcataacggagtgatcgcatagggataacagggtaatg ttaggctggagctgcttc 3'
OC 171	5' taaactgacgattcaacttataatctttgaaataatagtcggtatgaatacctccttag 3'
OC 436	5' attcgatactattcctgtgtaactttctaaggaacgagatagggataacagggtaattgtg taggctggagctgcttc 3'
OC 437	5' agataattctctggcgaaccacaccttaagggtgggtttgcgtatgaatacctcctta 3'
OC 780	5' agaaattaccgtcaccgccagttaatccggagagtcagcgtagggataacagggtaat gtgtaggctggagctgcttc 3'
OC 781	5' gcacgccagtcgggtcgccccatctcagcgcagtttcacatatgaatacctccttag 3'
OC 1097	5' caggagaagatgatgagttatcagccacaaaccgaagccgtagggataacaggg taatgttaggctggagctgcttc 3'
OC 1094	5' tgcgcagcgtttaccgccttctcattcagaaaacgcatatgaatacctccttag 3'
JL 118	5' atgatgaagagcgtccgatg 3'
JL 119	5' tgcgacggtgttgagcggg 3'

#### Extended Data Figure 10. Plasmids and primers used in this study

See supplemental information for references.

## Supplementary Material

Refer to Web version on PubMed Central for supplementary material.

## Acknowledgments

We thank Alasdair Gordon, Greg Ira, David Bates, Herman Dierick, Gadi Shaulsky and Ana Barker for critical comments; Ian Campbell's assistance with figure design; Ralf Nehring and Mohan Joshi for technical help; Sue Amundsen, Wilma Ross, Ana Šimatovi, Christian Rudolph, Max Gottesman, Jade Wang and Anthony Poteete for sharing strains. The study was supported by the NIH grant R01-GM088653 (C.H), the DLCC and P30 CA125123 Pilot grant (C.H, S.M.R), a gift from the WM Keck Foundation (S.M.R), the NIH grants R35-GM122598 and DP1-CA174424 (S.M.R), the NIH grant RO1-GM082837 (I.G), NSF PHY 1147498, PHY 1430124, PHY 1427654 (I.G), the Welch Foundation (Q-1759) and the John S. Dunn Foundation (I.G).

## References

1. Hersh MN, Ponder RG, Hastings PJ, Rosenberg SM. Adaptive mutation and amplification in *Escherichia coli*: two pathways of genome adaptation under stress. *Res Microbiol.* 2004; 155:352–359. [PubMed: 15207867]

2. Dillingham MS, Kowalczykowski SC. RecBCD enzyme and the repair of double-stranded DNA breaks. *Microbiol Mol Biol Rev.* 2008; 72:642–671. [PubMed: 19052323]
3. Dixon DA, Kowalczykowski SC. The recombination hotspot Chi is a regulatory sequence that acts by attenuating the nuclease activity of the *E coli* RecBCD enzyme. *Cell.* 1993; 73:87–96. [PubMed: 8384931]
4. Anderson DG, Kowalczykowski SC. The translocating RecBCD enzyme stimulates recombination by directing RecA protein onto ssDNA in a Chi-regulated manner. *Cell.* 1997; 90:77–86. [PubMed: 9230304]
5. Finkelstein IJ, Visnapuu ML, Greene EC. Single-molecule imaging reveals mechanisms of protein disruption by a DNA translocase. *Nature.* 2010; 468:983–987. [PubMed: 21107319]
6. Park JS, Marr MT, Roberts JW. *E coli* Transcription repair coupling factor (Mfd protein) rescues arrested complexes by promoting forward translocation. *Cell.* 2002; 109:757–767. [PubMed: 12086674]
7. Epshtein V, et al. UvrD facilitates DNA repair by pulling RNA polymerase backwards. *Nature.* 2014; 505:372–377. [PubMed: 24402227]
8. Erie DA, Hajiseyedjavadi O, Young MC, von Hippel PH. Multiple RNA polymerase conformations and GreA: control of the fidelity of transcription. *Science.* 1993; 262:867–873. [PubMed: 8235608]
9. Komissarova N, Kashlev M. Transcriptional arrest: *Escherichia coli* RNA polymerase translocates backward, leaving the 3' end of the RNA intact and extruded. *Proc Natl Acad Sci USA.* 1997; 94:1755–1760. [PubMed: 9050851]
10. Borukhov S, Sagitov V, Goldfarb A. Transcript cleavage factors from *E. coli*. *Cell.* 1993; 72:459–466. [PubMed: 8431948]
11. Koulich D, et al. Domain organization of *Escherichia coli* transcript cleavage factors GreA and GreB. *J Biol Chem.* 1997; 272:7201–7210. [PubMed: 9054416]
12. Paul BJ, et al. DksA: a critical component of the transcription initiation machinery that potentiates the regulation of rRNA promoters by ppGpp and the initiating NTP. *Cell.* 2004; 118:311–322. [PubMed: 15294157]
13. Tehrani AK, et al. The transcription factor DksA prevents conflicts between DNA replication and transcription machinery. *Cell.* 2010; 141:595–605. [PubMed: 20478253]
14. Vinella D, Potrykus K, Murphy H, Cashel M. Effects on growth by changes of the balance between GreA, GreB, and DksA suggest mutual competition and functional redundancy in *Escherichia coli*. *J Bacteriol.* 2012; 194:261–273. [PubMed: 22056927]
15. Ponder RG, Fonville NC, Rosenberg SM. A switch from high-fidelity to error-prone DNA double-strand break repair underlies stress-induced mutation. *Mol Cell.* 2005; 19:791–804. [PubMed: 16168374]
16. Amundsen SK, Taylor AF, Smith GR. The RecD subunit of the *Escherichia coli* RecBCD enzyme inhibits RecA loading, homologous recombination, and DNA repair. *Proc Natl Acad Sci USA.* 2000; 97:7399–7404. [PubMed: 10840065]
17. Morimatsu K, Kowalczykowski SC. RecFOR proteins load RecA protein onto gapped DNA to accelerate DNA strand exchange: a universal step of recombinational repair. *Mol Cell.* 2003; 11:1337–1347. [PubMed: 12769856]
18. Oppenheim AB, Kobiler O, Stavans J, Court DL, Adhya S. Switches in bacteriophage lambda development. *Annu Rev Genet.* 2005; 39:409–429. [PubMed: 16285866]
19. Friedberg, EC., Walker, GC., Siede, W., Wood, R., Schultz, R. DNA Repair and Mutagenesis. 2. ASM Press; 2006.
20. Kamarthapu V, et al. ppGpp couples transcription to DNA repair in *E. coli*. *Science.* 2016; 352:993–996. [PubMed: 27199428]
21. Potrykus K, Cashel M. (p)ppGpp: still magical? *Annu Rev Microbiol.* 2008; 62:35–51. [PubMed: 18454629]
22. Ross W, Vrentas CE, Sanchez-Vazquez P, Gaal T, Gourse RL. The magic spot: a ppGpp binding site on *E coli* RNA polymerase responsible for regulation of transcription initiation. *Mol Cell.* 2013; 50:420–429. [PubMed: 23623682]

23. Ross W, et al. ppGpp binding to a site at the RNAP-DksA interface accounts for its dramatic effects on transcription initiation during the stringent response. *Mol Cell*. 2016; 62:811–823. [PubMed: 27237053]
24. Kuzminov A. Collapse and repair of replication forks in *Escherichia coli*. *Mol Microbiol*. 1995; 16:373–384. [PubMed: 7565099]
25. Motamedi MR, Szigety SK, Rosenberg SM. Double-strand-break repair recombination in *Escherichia coli*: physical evidence for a DNA replication mechanism *in vivo*. *Genes Dev*. 1999; 13:2889–2903. [PubMed: 10557215]
26. Churchill JJ, Anderson DG, Kowalczykowski SC. The RecBC enzyme loads RecA protein onto ssDNA asymmetrically and independently of Chi, resulting in constitutive recombination activation. *Genes Dev*. 1999; 13:901–911. [PubMed: 10197989]
27. Anderson DG, Churchill JJ, Kowalczykowski SC. A single mutation, RecB(D1080A) eliminates RecA protein loading but not Chi recognition by RecBCD enzyme. *J Biol Chem*. 1999; 274:27139–27144. [PubMed: 10480929]
28. Ivancic-Bace I, et al. RecFOR function is required for DNA repair and recombination in a RecA loading-deficient *recB* mutant of *Escherichia coli*. *Genetics*. 2003; 163:485–494. [PubMed: 12618388]
29. Spies M, et al. A molecular throttle: the recombination hotspot Chi controls DNA translocation by the RecBCD helicase. *Cell*. 2003; 114:647–654. [PubMed: 13678587]
30. Garcia-Rubio M, et al. Different physiological relevance of yeast THO/TREX subunits in gene expression and genome integrity. *Mol Genet Genomics*. 2008; 279:123–132. [PubMed: 17960421]
31. Jeon C, Agarwal K. Fidelity of RNA polymerase II transcription controlled by elongation factor TFIIS. *Proc Natl Acad Sci USA*. 1996; 93:13677–13682. [PubMed: 8942993]
32. Hutchison CA III, et al. Design and synthesis of a minimal bacterial genome. *Science*. 2016; 351:aad6253. [PubMed: 27013737]
33. Gordon AJ, Satory D, Halliday JA, Herman C. Heritable change caused by transient transcription errors. *PLoS Genet*. 2013; 9:e1003595. [PubMed: 23825966]
34. Vermulst M, et al. Transcription errors induce proteotoxic stress and shorten cellular lifespan. *Nat Commun*. 2015; 6:8065. [PubMed: 26304740]
35. Krisko A, Radman M. Biology of extreme radiation resistance: the way of *Deinococcus radiodurans*. *Cold Spring Harb Perspect Biol*. 2013:5.

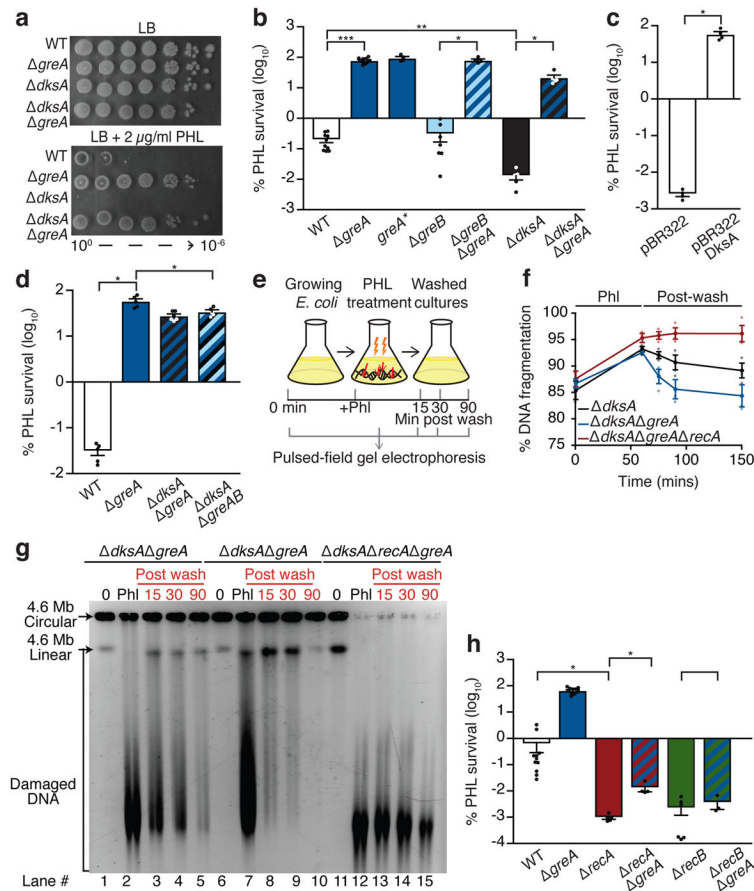


### Figure 1. GreA-RNAP interaction affects RecA-dependent break repair

a, Representative image (1/6) of serially diluted log cultures at the indicated phleomycin (PHL) concentrations. b–d,h, Quantitative PHL (2  $\mu g/ml$ ) survival of denoted mutants, n = 3 biological replicates (cultures), mean  $\pm$  s.e.m.;  $p < 0.001$  (\*\*\*),  $p < 0.01$  (\*\*),  $p < 0.05$  (\*) (Kruskal-Wallis test with multiple testing correction). e, Pulsed-field gel electrophoresis (PFGE) experimental scheme. f, PFGE before PHL treatment (0), after 20  $\mu g/ml$  PHL exposure for 60 min (Phl) and after washing PHL (post wash). g, PFGE quantification, mean  $\pm$  s.e.m.; n = 3 biological replicates (cultures). For source data, see Supplementary Figure 1.

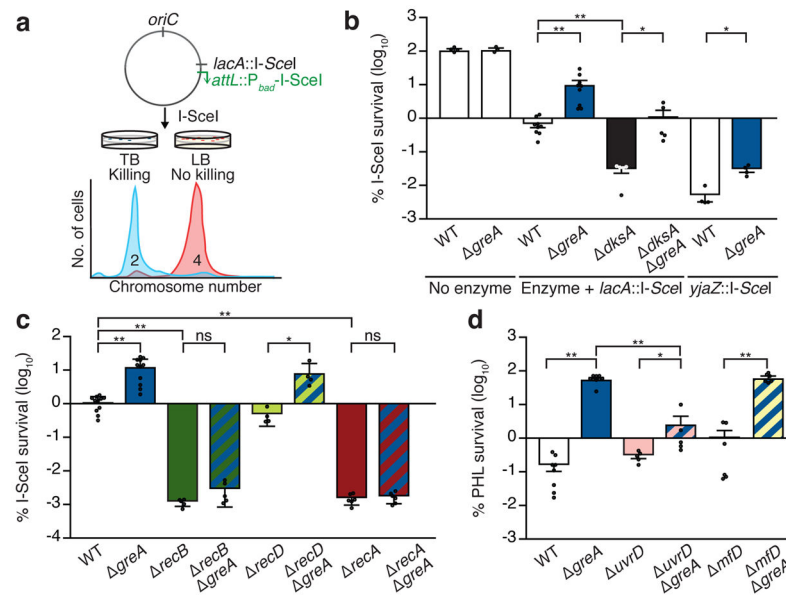


**Figure 2. Backtracked RNAP increases DSB resistance via the RecB pathway**

a, Scheme of I-SceI DSB survival assay with mock DNA content plot depicting chromosome copy number in TB vs. LB media. b, Survival after I-SceI cutting at *lacA*, no enzyme control containing *lacA* cutsite only and *yjaZ* loci. c, *lacA::I-SceI* DSB survival of indicated mutants. d, Phleomycin (PHL, 1µg/ml) survival of indicated mutants. For b–d, n = 3 biological replicates (cultures), mean ± s.e.m;  $p < 0.001$  (\*\*\*),  $p < 0.01$  (\*\*),  $p < 0.05$  (\*) (Kruskal-Wallis test with multiple testing correction).

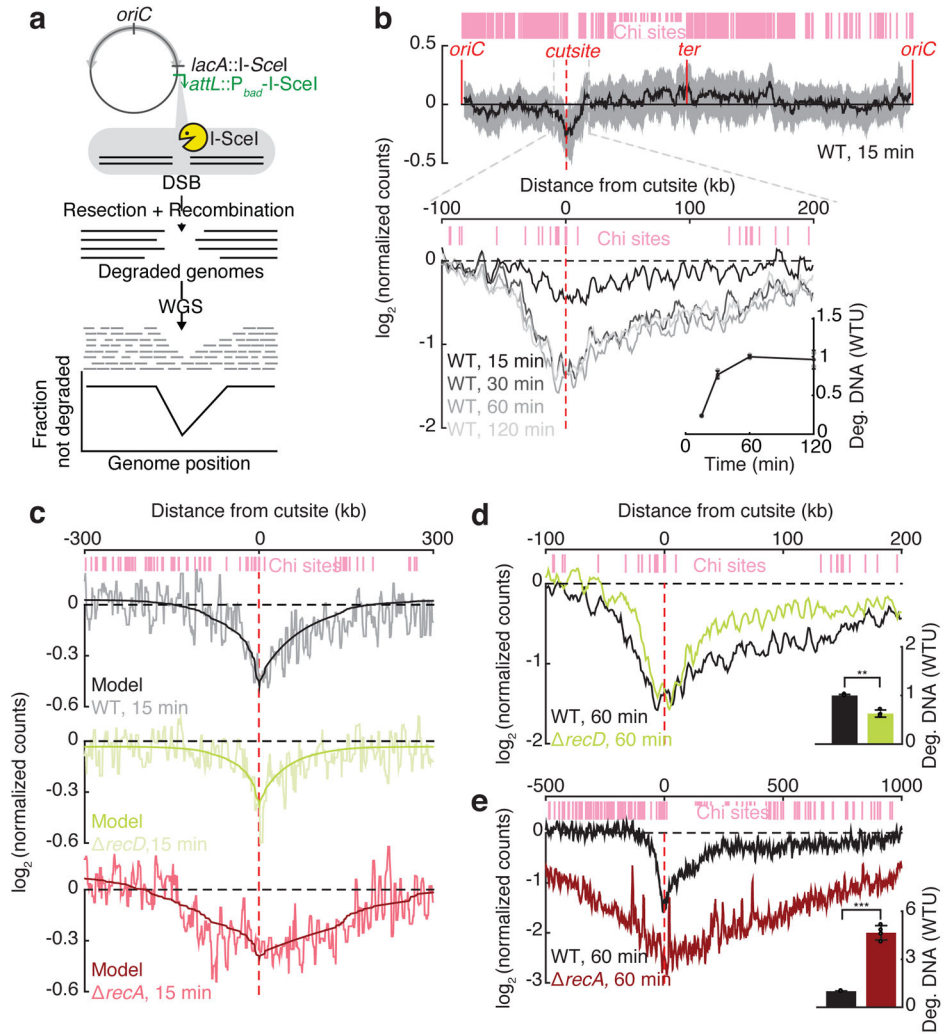


**Figure 3. XO-Seq**

a, XO-Seq combines I-SceI DSB induction and whole genome sequencing to generate reads reflecting repair processes. b, Timed degradation in wild-type (WT) cells, inset graph from  $n = 2$  biological replicates (cultures), mean  $\pm$  s.d; Deg. DNA (WTU) is genome degradation relative to WT in wild-type units. c, Mathematical modeling of RecBCD fitted to WT, *recD* and *recA* degradation curves (15 min). d, e, XO-Seq in *recD* (d) and *recA* (e) mutants; representative curves (1/3) shown; inset bar plots are  $n = 3$  biological replicates (cultures), mean  $\pm$  s.d;  $p < 0.001$  (\*\*\*),  $p < 0.01$  (\*\*). (Two-tailed two sample *t*-test).



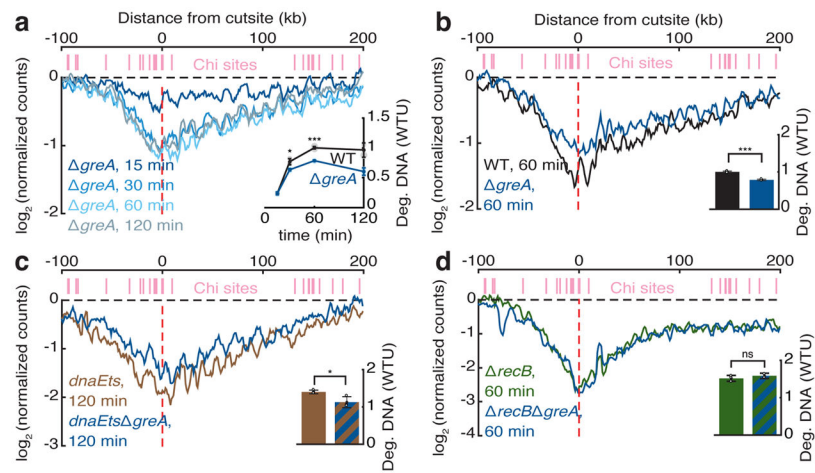


#### Figure 4. GreA interferes with DSB processing by RecB

a, Representative (1/2) temporal degradation in *greA* cells (DSB at *lacA*), inset graph from  $n = 2$  biological replicates (cultures). b–d Representative (1/2) degradation in indicated mutants at the denoted times (DSB at *lacA*). For a–d, inset plots are from  $n = 2$  biological replicates (cultures), mean  $\pm$  s.d;  $p < 0.001$  (\*\*\*),  $p < 0.05$  (\*),  $p > 0.05$  (ns) (Two-tailed two sample *t*-test). Deg. DNA (WTU) is genome degradation relative to WT in wild-type units.

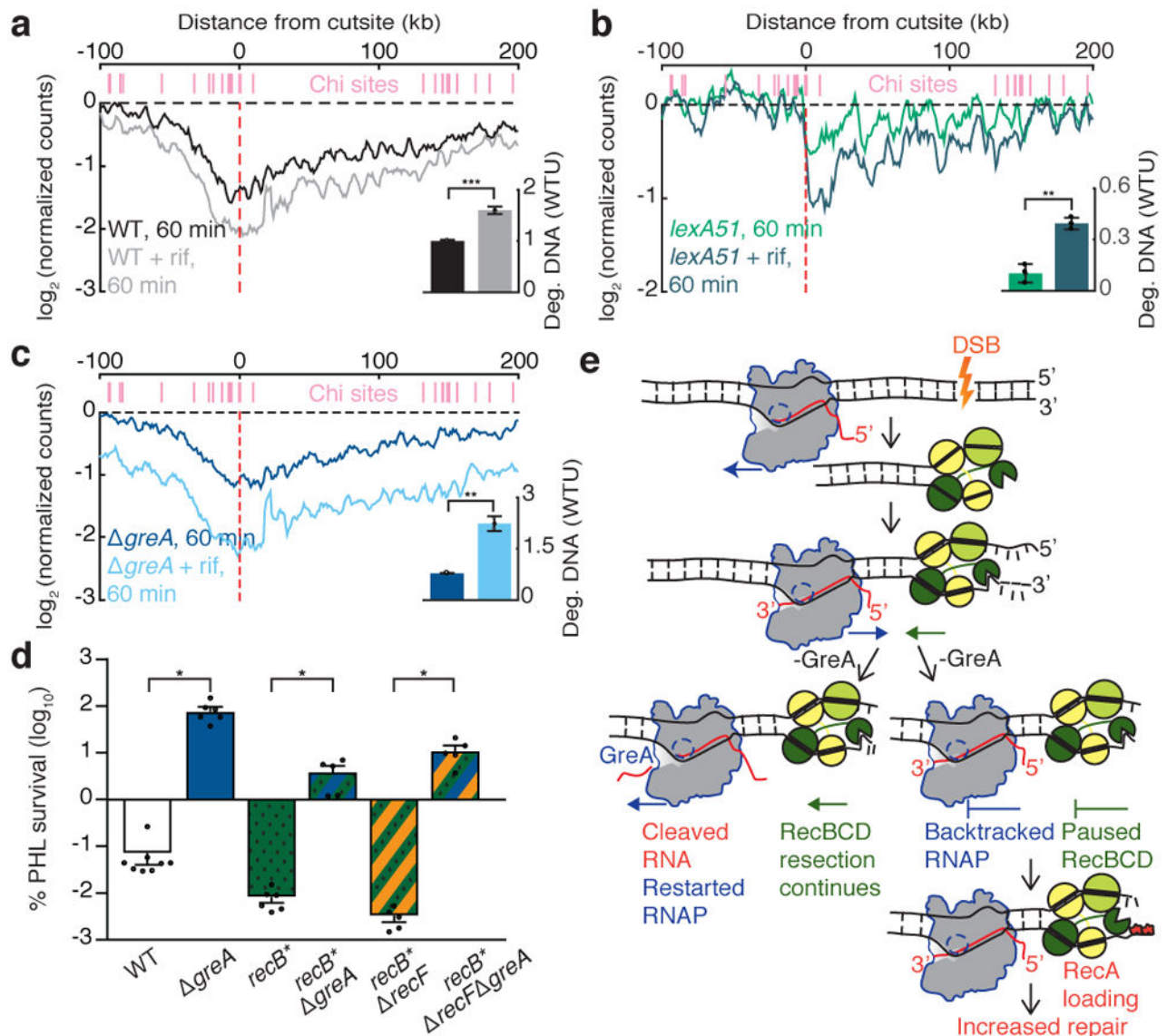


**Figure 5. Backtracked RNAP promotes recombination by increasing RecA loading**

a–c, Representative (1/2) XO-Seq plots (DSB at *lacA* and rifampicin (rif) addition) in the indicated strains, inset plots are  $n = 2$ ; mean  $\pm$  s.d.;  $p < 0.001$  (\*\*\*) ,  $p < 0.01$  (\*\*) (Two-tailed two sample *t*-test); Deg. DNA (WTU) is genome degradation relative to WT in wild-type units. d, Phleomycin (PHL, 1  $\mu$ g/ml) survival of indicated mutants,  $n = 3$  biological replicates (cultures), mean  $\pm$  s.e.m.;  $p < 0.01$  (\*\*) (Kruskal-Wallis test with multiple testing correction). e, Model describing how backtracked RNAP formation can enhance DSB repair by altering RecBCD function and promoting RecA loading.